ELSEVIER

International Journal of Mass Spectrometry 201 (2000) 233–244

International Journal of Mass Spectrometry

Energy transfer pathways in the collisional activation of peptides

Oussama Meroueh, William L. Hase*

Department of Chemistry, Wayne State University, Detroit, MI 48202-3489, USA

Received 6 December 1999; accepted 22 December 1999

Abstract

Classical trajectory simulations were carried out to study details of the energy transfer mechanism for activation of polyglycine $(gly)_n$ and polyalanine $(ala)_n$ peptide ions via collisions with Ar atoms. The Amber valence force field was used to represent the peptide intramolecular potential and the argon–peptide interaction was modeled using parameters previously determined from high level ab initio calculations. Energy transfer was studied versus collision impact parameter *b*, the collision energy, and peptide temperature and structure. Energy transfer to rotation becomes important for extended peptides at large *b*, but with averaging over impact parameter is smaller than transfer to vibration. Specific pathways for vibrational energy transfer were distinguished by determining the efficiency of energy transfer with various combinations of low and high frequency modes constrained. With all stretching and bending modes constrained the efficiency of energy transfer is more than 80% of that without constraints, which illustrates the efficient excitation of the torsional modes. Varying the peptide structure has a significant effect on the energy transfer efficiency, with larger energy transfer for the folded structures. The efficiency of energy transfer increases with increase in collisional energy. (Int J Mass Spectrom 201 (2000) 233–244) © 2000 Elsevier Science B.V.

Keywords: Energy transfer pathways; Peptides

1. Introduction

Numerous experimental techniques have been used to study the collision induced dissociation (CID) of peptides in the gas phase [1–5]. Ion mobility studies have provided information about the structures of the peptides [6–11]. Theoretical/computational methods, including classical trajectory simulations [12–14], Rice-Ramsperger-Kassel-Marcus (RRKM) theory [2,3] and electronic structure theory [15–19], have been used to interpret and analyze these CID experiments. CID is generally regarded as a two-step process [20]. Energy is first transferred into internal vibrational and rotational states of the peptide ion, which subsequently undergoes unimolecular dissociation when its internal energy exceeds the dissociation limit. The collisional activation step thus becomes an important part of the dissociation process. Recent studies [1–3,12,14] have found that the energy transfer efficiency is dependent on several factors including the initial translational energy, the size of the peptide, and also the peptide structure. The collider mass also plays an important role in the collision activation process, where heavy colliders such as Kr and Xe tend to transfer energy much more efficiently; i.e. as much as 80% of the initial translational energy [12].

* Corresponding author. E-mail: WLH@CHEM.WAYNE.EDU

PII S1387-3806(00)00229-3

Several mechanisms have been proposed for CID of peptides in the gas phase. Levine and co-workers [21] have proposed a model based on migration of electronic excitation where the charge migrates to the reactive site and allows for peptide fragmentation. For protonated peptides, the mobile proton model [1,22] was proposed to explain peptide fragmentation patterns. The proton is thought to migrate from the N-terminus, its most preferred site [23], to the various groups along the peptide and subsequently leading the peptide toward a specific dissociation pathway [15,16,19]. For large peptides it is still not clear whether the proton migrates to the most basic site, the fragmentation site or at any site in a random fashion as was proposed by Harrison and Yalcin [24]. Whether the peptide fragmentation is due to charge or proton transfer, the peptide's highly flexible backbone facilitates charge and proton transfer [1,2] and, therefore, the peptide's conformation becomes an important aspect of the collision process.

During a collision, energy stored in translational motion is converted into internal vibrational and rotational energies of the substrate. Classical trajectory simulations enable one to study in detail the extent of energy transfer and how the energy transferred is distributed in a substrate. Several simulation studies have been carried out of the deactivation of highly excited polyatomic molecules [25–28]. Classical trajectory simulations on argon and benzene collisions have shown that replacing the hydrogens by deuterium increases the energy transfer efficiency, suggesting that low frequency modes are an important part of the collision efficiency [26]. Furthermore, recent experiments on benzene and toluene [29] and simulations of the collisional energy transfer in ethane [30] have shown that torsional motions, which are an important part of peptide dynamics, play an important role in the energy transfer process.

A previous trajectory simulation provided detailed information concerning the energy transfer dynamics for Ar collisions with polyglycine $(gly)_n$ and polyalamine $(ala)_n$ ions [12]. The work presented here addresses several important questions raised by this study. They include the relative importance of rotational and vibrational energy transfer in the collision activation, identification of the vibrational modes initially excited in the collisional activation, and the effect of protein structure on the energy transfer efficiency.

2. Computational details

The trajectory simulations were performed with the general molecular dynamics package VENUS96 [31], as described previously [12]. The potential energy function is represented as

$$V = V_{\text{peptide}} + V_{\text{Ar,peptide}} \tag{1}$$

where V_{peptide} is the protonated peptide intramolecular potential and $V_{\text{Ar,peptide}}$ is the Ar–peptide intermolecular potential. The former is the Amber valence force field of Cornell et al. [32] and is expressed as

$$V_{\text{peptide}} = \sum_{\text{bonds}} K_r(r - r_{\text{eq}})^2 + \sum_{\text{angles}} K_\theta(\theta - \theta_{\text{eq}})^2 + \sum_{\text{dihedrals}} \frac{V_n}{2}[a - \cos(n\phi - \gamma)] + \sum_{i>j} [A_{ij}/r_{ij}^{12} - B_{ij}/r_{ij}^6 + q_i q_j/(\epsilon r_{ij})] \tag{2}$$

The Ar–peptide intermolecular potential is represented by a sum of two-body potentials, fit to QCISD(T)/6-311++G** ab initio calculations for Ar interacting with small molecules representative of peptide functional groups [12].

Initial conditions for protonated $(gly)_n$ and $(ala)_n$ peptides were chosen by adding a quasiclassical 300 K Boltzmann distribution of vibrational/rotational energies to a potential energy minimum of the protonated peptide [12,33–36]. The folded and extended structures of $(gly)_4$ used for the simulations are shown in Fig. 1. Included with each structure is its radius of gyration defined by

$$r_g = \sqrt{\frac{\sum r_i^2}{n+1}} \tag{3}$$

where the r_i's are the distances of the n atoms from the peptide's center of mass. Simulations were also performed for different initial structures of $(gly)_6$ and

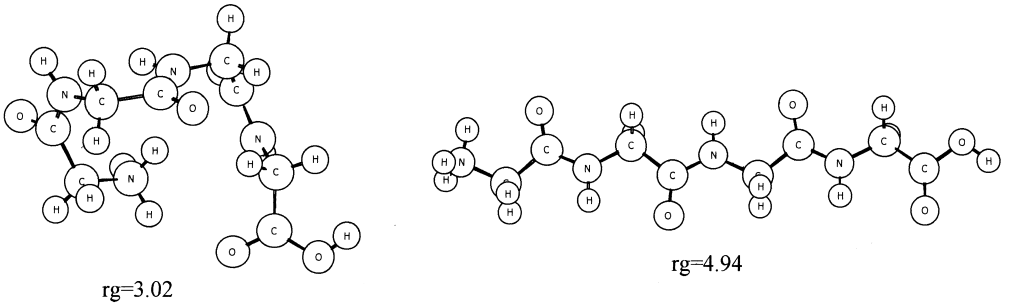

Fig. 1. Folded and extended $(gly)_4$ structures used in the simulations.

$(ala)_5$. The polyalanine peptides differ from the polyglycines in that a backbone H atom of the latter is replaced by a CH_3 group. A range of folded and extended structures were determined for these peptides by running trajectories at 3000 K and then quenching the trajectories at random time intervals into the different potential minima they accessed. Their structures and radii of gyration are given in Figs. 2 and 3.

After adding the vibrational/rotational energy, the peptide was randomly rotated about its Euler angles [37]. Relative velocities were then added to Ar and the peptide in accord with the center-of-mass collision energy and the collision impact parameter [37]. The impact parameter b was either set to a specified value or chosen randomly between 0 and b_{max}. The criterion for selecting the maximum impact parameter b_{max} is described below.

Trajectories are initiated and stopped at distances large enough to guarantee no interaction between the peptide and the argon atom. The property determined from the trajectories is the amount of relative translational energy transferred to the peptide in the form of rotational and vibrational energies. The former is calculated from

$$E_{rot} = \frac{1}{2}\,\omega \cdot \mathbf{j} \qquad (4)$$

where ω is the peptide's angular velocity and $\mathbf{j}$ is its angular momentum. The final E_{rot} is determined by averaging over 10 fs of the peptide's motion. The rotational energy transfer is the difference in the final and initial values of E_{rot}; i.e. $\Delta E_{rot} = E^f_{rot} - E^i_{rot}$. The vibrational energy transfer ΔE_{vib} is then the total energy transfer minus ΔE_{rot}. To study the dynamics of this energy-transfer process, the relative translational energy, the energy of the peptide, and the peptide structure were analyzed as a function of time. Uncertainties in the reported results are the standard deviation in the mean [38], which is the standard deviation divided by the square root of the total number of trajectories. Five hundred trajectories were calculated for each initial condition studied unless otherwise stated.

3. Results

3.1. Ensemble averaged energy transfer and peptide conformational dynamics

In these simulations, energy transfer as a result of Ar plus peptide ion collisions is studied versus the peptide structure. An ensemble of peptide ions at temperature T with a specific structure is sampled by adding $RT/2$ to each of the peptide's external rotation axis and selecting the peptide's vibrational energy from its normal mode Boltzmann distribution. Since the peptides have low energy pathways for conformational changes [39], it is necessary to insure the peptide retains its initial structure before it collides with Ar. This was investigated for trajectory initial conditions with a peptide temperature of 300 K, a

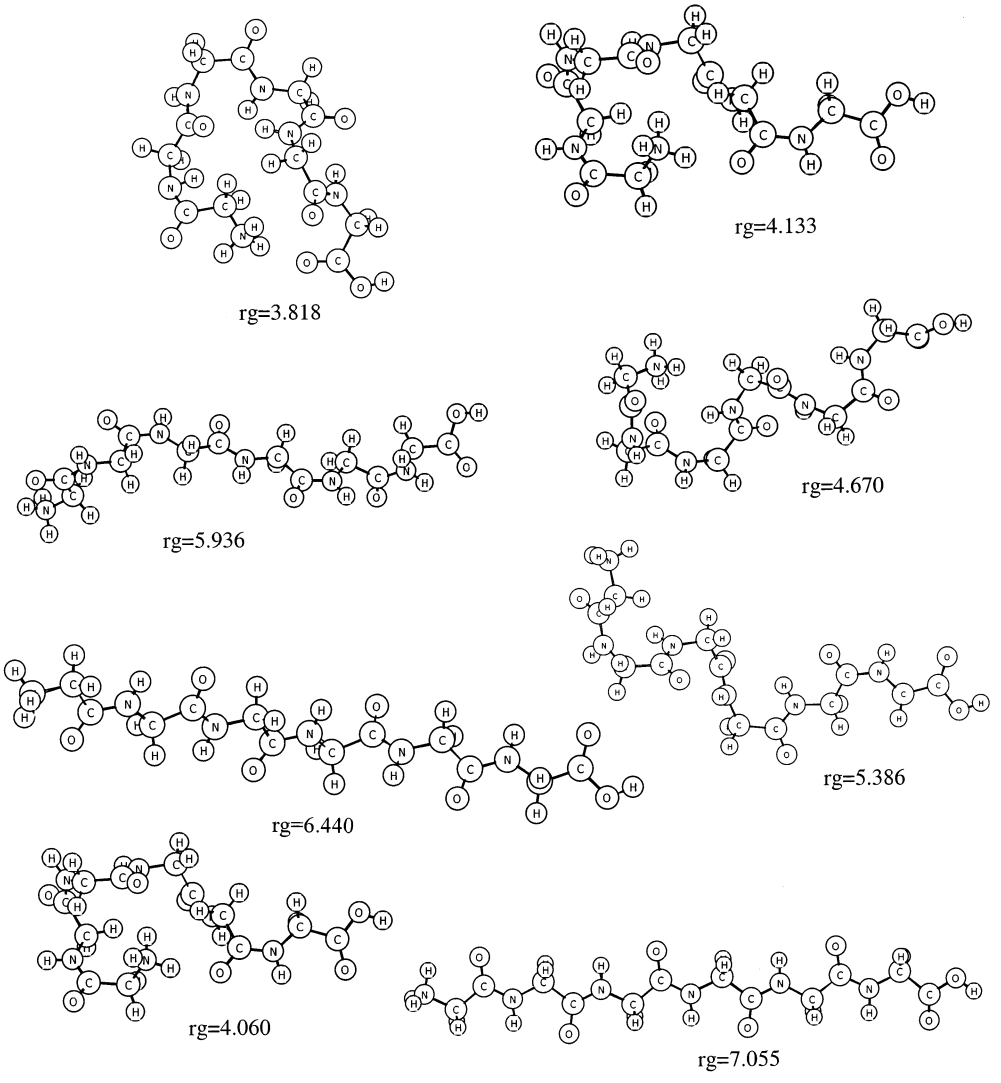

Fig. 2. Structures and radii of gyration of $(gly)_6$ peptides used in the simulations.

relative translational energy E_{rel} of 100 kcal/mol, and an impact parameter of 0 Å. The average radius of gyration and the average peptide internal energy were calculated versus time for an ensemble of 200 trajectories. Results for the folded and extended structures of $(gly)_4$ are given in Fig. 4.

As a result of a collision with Ar, the average change in the peptide's internal energy is 61 and 56 kcal/mol for the folded and unfolded peptide structures, respectively. There is no change in the internal energy without a collision. For the extended peptide the average radius of gyration is nearly constant up to the time of the collision, at which the increase in the peptide's internal energy causes a pronounced decrease in the average r_g as a result of folding. For the folded peptide there is a small ~0.2 Å increase in the average r_g up to the time of the collision, indicating the peptide is on average undergoing a small amount of unfolding. When the peptide's internal energy has been increased, as a result of the collision, the

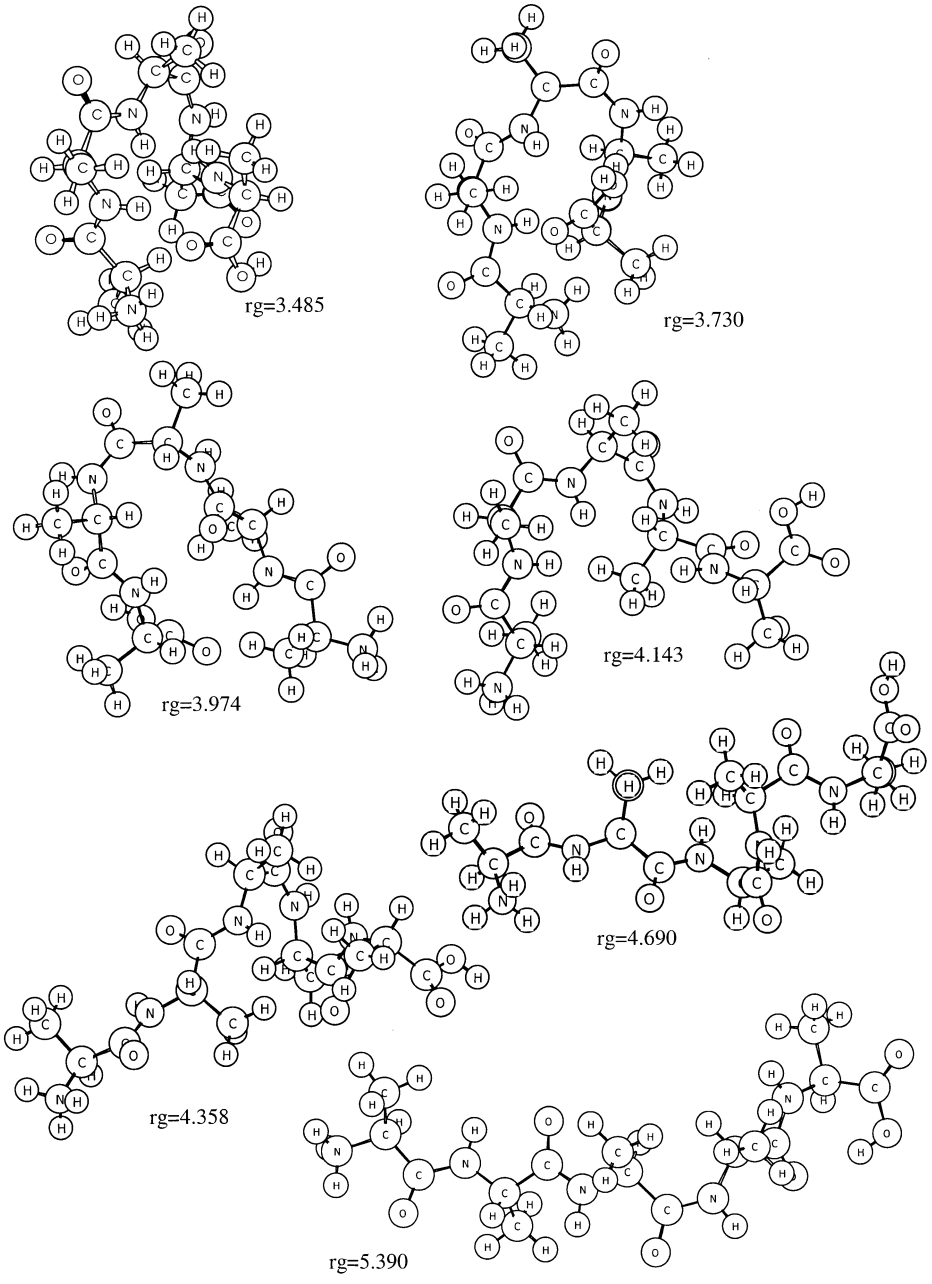

Fig. 3. Structures and radii of gyration of $(ala)_5$ peptides used in the simulations.

increase in average r_g and, thus, unfolding of the peptide becomes more rapid.

An important result from Fig. 4 is that the average peptide structure changes, at most, by only a small amount from the time the peptide is excited until the time it collides with Ar. Therefore, it is possible to study the dynamics of Ar + peptide energy transfer as a function of the peptide structure.

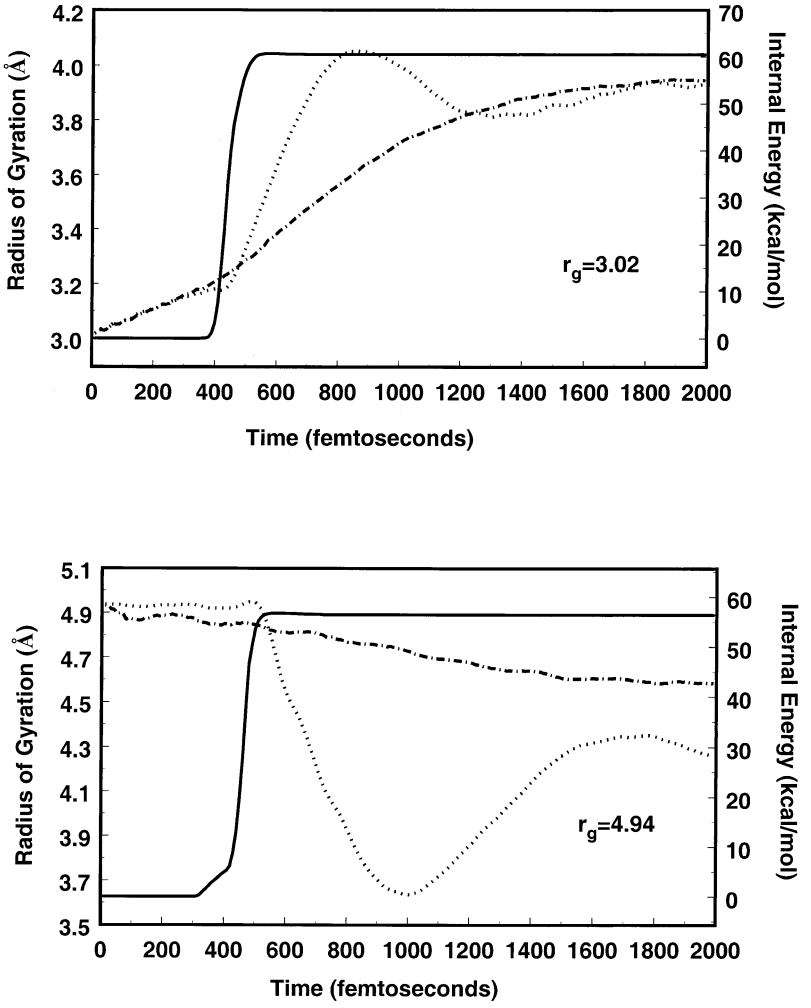

Fig. 4. Average radius of gyration and average peptide internal energy vs. time for ensembles of 200 initially folded (r_g = 3.02 Å) and extended (r_g = 4.94 Å) tetraglycine peptide ions, with a temperature of 300 K. Results are given for a collision of each peptide in the ensemble with Ar (E_{rel} = 100 kcal/mol and b = 0 Å) and for the same time period but without a collision. Average internal energy with Ar + peptide collision (solid line); average r_g with an Ar + peptide collision (dotted line); and average r_g without a collision (dashed-dotted line).

3.2. Relative importance of rotational and vibrational energy transfers

An important issue, in using RRKM theory to model peptide dissociation via collisional activation [2,3], is the relative amounts of rotational and vibrational energy transferred to the peptide. Vibrational energy is more efficient for promoting dissociation than is rotation [40]. In this work the percent energy transfer to rotation and vibration was studied for both the folded and extended $(gly)_4$ structures in Fig. 1. The peptide temperature was varied between 50 and 700 K, and E_{rel} in the range of 20–1000 kcal/mol was studied. The collision impact parameter was fixed at 0 Å, varied between 0 and b_{max}, and selected randomly between 0 and b_{max}.

3.2.1. b = 0 collisions

Values of percent total energy transfer ΔE and rotational and vibrational energy transfer, ΔE_{rot} and

Table 1
Percent energy transfer for folded and extended $(gly)_4$ structures[a]

	Folded		Extended	
Temperature[b] (K)	ΔE[c]	ΔE_{rot}	ΔE	ΔE_{rot}
		E_{rel} = 20 kcal/mol		
0	44.0 (0.9)	5.8 (0.4)	43.9 (1.0)	5.3 (0.3)
50	44.3 (0.9)	6.0 (0.4)	43.2 (1.0)	5.5 (0.3)
300	41.0 (0.6)	7.4 (0.3)	44.2 (0.9)	6.0 (0.3)
500	37.8 (0.8)	7.4 (0.4)	43.8 (1.0)	6.4 (0.3)
700	36.3 (1.1)	8.0 (0.5)	43.0 (0.9)	6.8 (0.4)
		E_{rel} = 100 kcal/mol		
0	59.6 (0.6)	4.0 (0.2)	54.7 (0.7)	4.3 (0.2)
50	59.7 (0.6)	4.1 (0.1)	55.1 (0.8)	4.5 (0.2)
300	58.4 (0.6)	4.7 (0.1)	54.3 (0.7)	4.5 (0.2)
500	58.1 (0.7)	4.8 (0.2)	54.1 (0.8)	4.5 (0.2)
700	56.8 (0.7)	4.6 (0.2)	52.8 (0.8)	4.4 (0.2)
		E_{rel} = 400 kcal/mol		
0	71.8 (0.4)	2.0 (0.1)	64.8 (0.8)	2.2 (0.1)
50	72.9 (0.4)	1.8 (0.1)	64.6 (0.8)	2.2 (0.1)
300	72.4 (0.4)	1.9 (0.1)	64.0 (0.8)	2.2 (0.1)
500	70.1 (1.1)	1.8 (0.2)	63.8 (0.8)	2.2 (0.1)
700	70.2 (0.8)	2.5 (0.2)	63.7 (0.8)	2.3 (0.2)
		E_{rel} = 1000 kcal/mol		
0	76.4 (0.5)	1.2 (0.1)	71.7 (0.8)	1.2 (0.1)
50	76.5 (0.5)	1.1 (0.1)	71.4 (0.8)	1.2 (0.1)
300	74.3 (0.6)	1.3 (0.1)	70.5 (0.8)	1.2 (0.1)
500	73.5 (1.0)	1.4 (0.1)	70.2 (0.8)	1.2 (0.1)
700	71.4 (1.0)	1.4 (0.1)	70.1 (0.8)	1.2 (0.1)

[a] Simulations are for an impact parameter of 0 Å. The peptide structures are in Fig. 1. The uncertainty, standard deviation of the mean, is given in parentheses.
[b] This is the peptide's vibrational temperature. The rotational temperature was fixed at 300 K.
[c] ΔE is for the percent total energy transfer.

ΔE_{vib}, are given in Table 1 for $b = 0$ collisions, with the vibrational temperature of the peptide varied and E_{rel} in the range of 20–1000 kcal/mol. The initial rotational temperature of the peptide was fixed at 300 K. Rotational energy transfer makes only a minor contribution to the total energy transfer for these collisions. The temperature of the peptide has a negligible effect on the energy transfer efficiency, except for the lowest E_{rel} of 20 kcal/mol. In contrast, energy transfer is strongly influenced by the collision energy. The efficiency is near 40% for E_{rel} = 20 kcal/mol, but increases with increase in E_{rel}, becoming 75% for folded $(gly)_4$ at E_{rel} = 1000 kcal/mol. Such a change in energy transfer efficiency is consistent with a statistical type energy transfer at low E_{rel} [41] and the energy transfer becoming impulsive at higher E_{rel} [12].

3.2.2. Effect of impact parameter

The effect of impact parameter on the energy transfer efficiency, for the folded and extended $(gly)_4$ peptides, is shown in Fig. 5 for collisions with E_{rel} of 100 kcal/mol and a peptide temperature of 300 K. At small impact parameter the energy transfer is primarily to vibration with transfer to rotation becoming more important as the impact parameter is increased. For the extended structure, energy transfer to rotation and vibration become similar at the larger impact parameters.

For the extended peptide energy transfer becomes

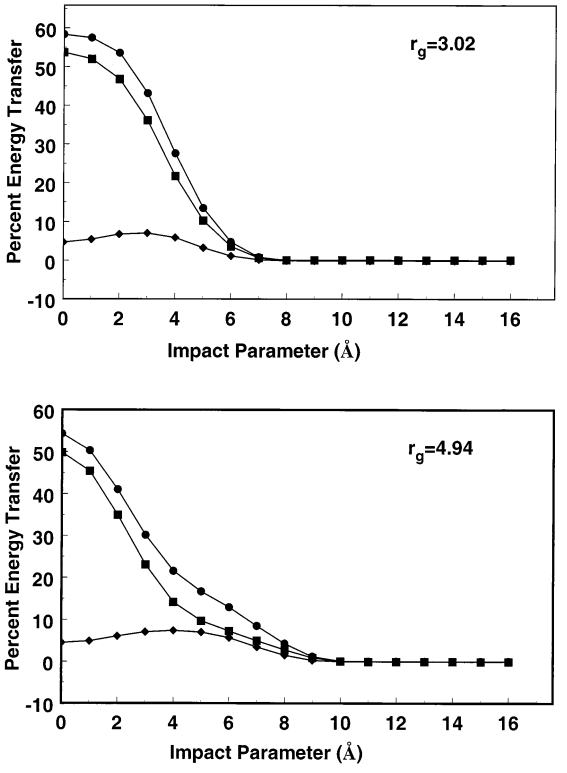

Fig. 5. Total percent energy transfer (circle) and percent energy transfer to vibration (square) and rotation (diamond) vs. impact parameter for collisions with E_{rel} = 100 kcal/mol and $T_{peptide}$ = 300 K. Results for the folded (r_g = 3.02 Å) and extended (r_g = 4.94 Å) $(gly)_4$ peptides.

negligible at b of ~10 Å, whereas for the more compact peptide it becomes negligible at ~7 Å. These are approximate values for b_{max}. A more quantitative approach for specifying b_{max} from Fig. 5 is to weight the average energy transfer versus impact parameter $\langle \Delta E(b) \rangle$ by the differential cross section $2\pi b\ db$ to find

$$\langle \Delta E \rangle_\sigma = \int_0^\infty \langle \Delta E(b) \rangle 2\pi b\ db \qquad (5)$$

which is a quantity converged from the trajectory simulations [42]. It is similar for the two structures, and equals 3638 and 3207 kcal Å^2/mol for extended and folded $(gly)_4$, respectively. Values for b_{max} were deduced from Eq. (5) by setting the integral's upper

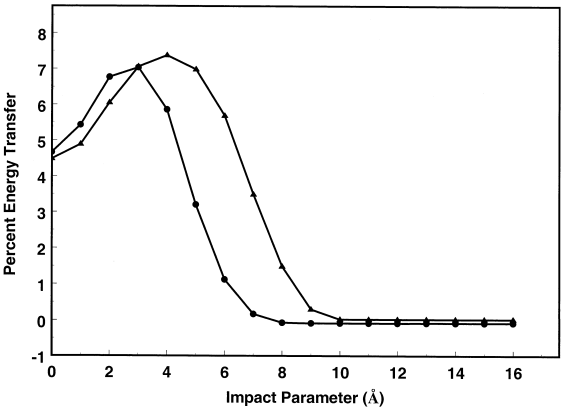

Fig. 6. Comparison of the percent rotational energy transfer plots in Fig. 5 for the folded (circle) and extended (triangle) $(gly)_4$ peptides.

limit to a value of b, which gives a $\langle \Delta E \rangle_\sigma$ value within 10^{-4} percent of the limiting value [43]. The resulting b_{max} is 10.2 and 7.6 Å for extended and folded $(gly)_4$, respectively. Nearly identical b_{max} values are found by using a fitting criterion of 1 or 10^{-2} percent.

A value for $\langle \Delta E \rangle$, averaged over b, may be determined by dividing $\langle \Delta E \rangle_\sigma$ by the collision cross section πb_{max}^2. Using the above b_{max} values, $\langle \Delta E \rangle$ is 11.1 and 17.5 kcal/mol for the extended and folded $(gly)_4$ peptides, respectively. Though $\langle \Delta E \rangle_\sigma$ is similar for the two structures, $\langle \Delta E \rangle$ is larger for the folded structure since it has a smaller cross section. Writing $\langle \Delta E(b) \rangle$ in Eq. (5) as the sum $\langle \Delta E_{vib}(b) \rangle + \langle \Delta E_{rot}(b) \rangle$ and taking $\langle \Delta E_{vib}(b) \rangle$ and $\langle \Delta E_{rot}(b) \rangle$ from Fig. 5, the average transfers to vibration and rotation, averaged over b, are found to be $\langle \Delta E_{vib} \rangle$ = 7.7 kcal/mol and $\langle \Delta E_{rot} \rangle$ = 3.4 kcal/mol for the extended peptide and $\langle \Delta E_{vib} \rangle$ = 14.5 kcal/mol and $\langle \Delta E_{rot} \rangle$ = 3.0 kcal/mol for the folded peptide. For the folded peptide $\langle \Delta E_{rot} \rangle$ is 4.8 times smaller than $\langle \Delta E_{vib} \rangle$, but for the extended peptide $\langle \Delta E_{rot} \rangle$ is only 2.3 times smaller. The plots of percent rotational energy transfer for the extended and folded $(gly)_4$ peptides are compared in Fig. 6. These percent rotational energy transfer values for extended $(gly)_4$ are somewhat smaller than the preliminary values reported previously [12]. A reanalysis of these previous percent rotational energy transfer values shows that

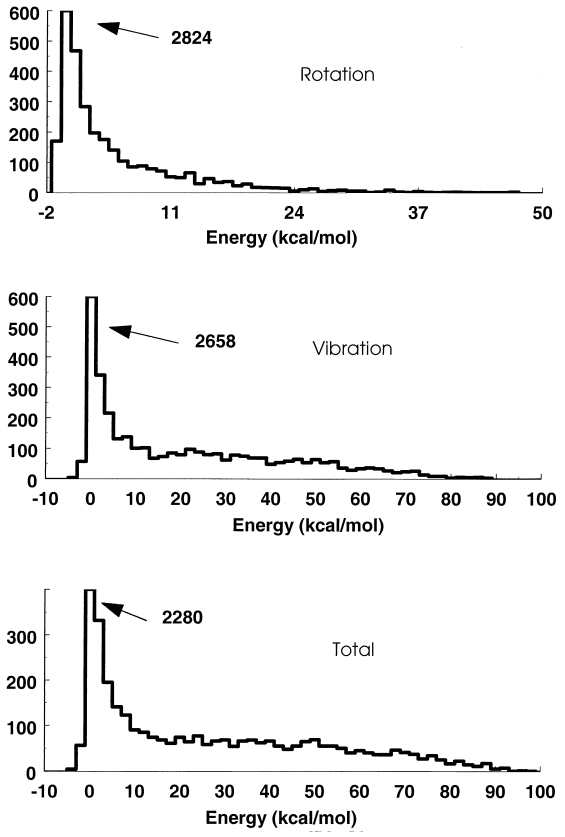

Fig. 7. Distributions of total energy transfer ΔE and vibrational and rotational energy transfer ΔE_{vib} and ΔE_{rot} for Ar collisions with folded $(gly)_4$ at E_{rel} = 100 kcal/mol and a peptide temperature of 300 K. The impact parameter is chosen randomly between 0 and b_{max}.

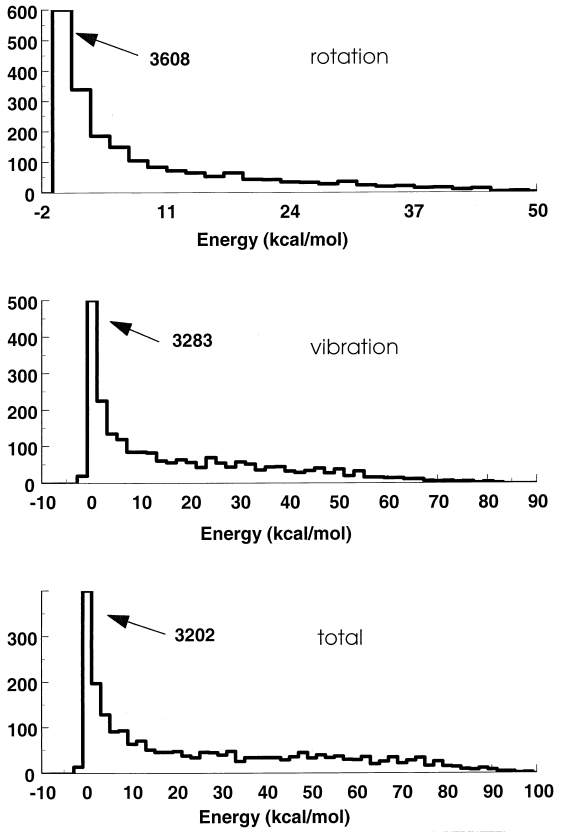

Fig. 8. Same as Fig. 7, but for the extended $(gly)_4$ peptide.

there was a mistake in the initial rotational energy of the peptide and, thus, the reported rotational energy transfer values are too large.

Distributions of ΔE, ΔE_{vib}, and ΔE_{rot} for the folded and extended $(gly)_4$ peptides, with b chosen randomly between 0 and b_{max}, are shown in Figs. 7 and 8, respectively. The collisions are for E_{rel} = 100 kcal/mol and a peptide temperature of 300 K. For both structures, there are collisions which transfer nearly all of E_{rel}. Because of the shape of the extended peptide and its larger b_{max} value, its distributions have more events centered around $\Delta E = 0$. As expected from the results in Fig. 6, the ΔE_{rot} distribution extends to higher energy transfer values for the extended peptide.

3.3. Effect of peptide structure on energy transfer

In previous work [12], the efficiency of energy transfer to the peptide was found to depend on peptide structure. As illustrated by the above $\langle \Delta E \rangle_\sigma$ and $\langle \Delta E \rangle$ values, the same effect is found here. A more comprehensive study of the effect of peptide structure on the energy transfer efficiency is shown in Fig. 9. Here the percent energy transfer for the $(gly)_6$ and $(ala)_5$ peptides in Figs. 2 and 3 are compared. These two peptides have a similar number of atoms; i.e. 46 and 54, respectively. The trend for each of these peptides is for the percent energy transfer to increase as the peptide's becomes more folded and its radius of gyration decreases. This effect is more pronounced for the $(ala)_5$ peptide, whose energy transfer efficiency increases by ~20% as its structure becomes more folded.

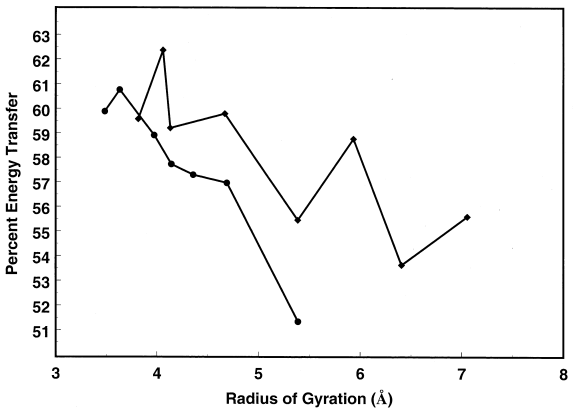

Fig. 9. Percent energy transfer for the $(gly)_6$ peptides in Fig. 2, (diamond), and the $(ala)_5$ peptides in Fig. 3, (circle). Calculations are for $b = 0$, $E_{rel} = 100$ kcal/mol and a peptide temperature of 300 K.

Independence of energy transfer on peptide structure and/or size is indicative of impulsive energy transfer [12]. Here the energy transfer dynamics is only influenced by the interaction of the Ar atom with the localized region of the peptide with which it collides. The weaker dependence of energy transfer on structure for $(gly)_6$ indicates the energy transfer dynamics for this peptide is nearer the impulsive limit than for $(ala)_5$. A similar result was observed previously [12] in comparing the effect of size on energy transfer for the extended $(gly)_n$ and $(ala)_n$ peptides. Energy transfer is more impulsive for the $(gly)_n$ peptides.

When averaged over impact parameter the extended and folded structures of $(gly)_4$ exhibit very similar energy transfer characteristics. This is illustrated in Fig. 10 where $\langle \Delta E \rangle_\sigma$, Eq. (5), for these peptides are plotted versus E_{rel}. Though these two structures have different cross sections πb_{max}^2 and average energy transfers $\langle \Delta E \rangle$, they have similar $\langle \Delta E \rangle \pi b_{max}^2$ values which are approximately 10% larger for the extended structure. The b_{max} value, determined as described above, decreases from 7.6 to 6.7 Å for the folded structure as E_{rel} is increased from 100 to 1000 kcal/mol and decreases from 10.2 to 9.3 Å for the extended structure with the same increase in E_{rel}. As discussed above, $\langle \Delta E_{rot} \rangle$ is a larger fraction of $\langle \Delta E \rangle$ for the extended structure.

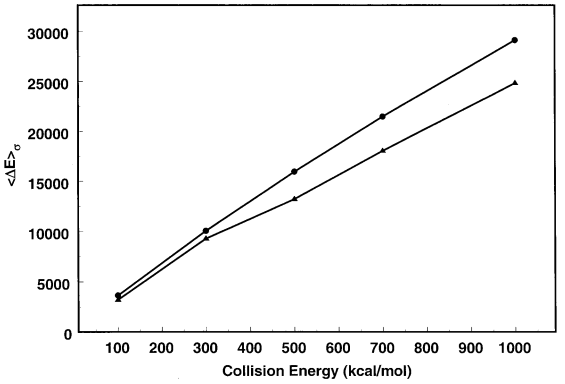

Fig. 10. The impact parameter averaged energy transfer $\langle \Delta E \rangle_\sigma$ in Eq. (5) for the extended (circle) and folded (triangle) $(gly)_4$ peptides vs. E_{rel}.

3.4. Mode specific energy transfer

The efficiency of energy transfer to specific modes of extended $(gly)_4$ was studied by constraining different sets of its internal coordinates. This was accomplished by increasing the force constants for the set of internal coordinates so that their vibrational modes are adiabatic during the collision and do not accept energy [44]. Using H to identify a heavy atom such as C, N, or O and L to identify the light hydrogen atom, the internal coordinates were grouped into the following eight sets; i.e. HL stretches, HH stretches, LHL bends, HHL bends, HHH bends, LHHL torsions, HHHL torsions, and HHHH torsions. The percent energy transfers with these different modes constrained are listed in Table 2. The calculations are for $E_{rel} = 100$ kcal/mol, $b = 0$, and the peptide initially in its classical potential energy minimum with no rotational energy. Initial conditions were also chosen by adding a quasiclassical 300 K Boltzmann distribution of vibrational/rotational energy to the potential energy minimum of the protonated peptide, as described in Sec. 2. This latter scheme for sampling the peptide's initial conditions gives energy transfer efficiencies to within 3.5% of the values in Table 2.

Constraining the stretches has the smallest effect on the energy transfer efficiency, while constraining the HHHL and HHHH torsions has the greatest effect. Constraining one set of these torsions lowers the

Table 2
Percent energy transfer to extended $(gly)_4$ with specific internal coordinates constrained[a]

Coordinates constrained[b]	$E_{rel} = 100$[c]
None	58 (4)[d]
HL stretches	56 (4)
HH stretches	56 (4)
All stretches	57 (4)
LHL bends	57 (5)
HHL bends	56 (5)
HHH bends	55 (5)
All bends	53 (5)
All bends and stretches	49 (6)
LHHL torsions	57 (4)
HHHL torsions	37 (9)
HHHH torsions	31 (9)
All bends and dihedrals	11 (11)
All	13 (13)

[a] The calculations are for $E_{rel} = 100$ kcal/mol, $b = 0$, and the peptide initially in its classical potential energy minimum.
[b] H corresponds to a heavy atom, i.e. C, N, or O. L corresponds to the light hydrogen atom.
[c] Energy is in kcal/mol.
[d] The standard deviation in the mean percent energy transfer is approximately 1%. The percent energy transfer to rotation is in parentheses.

percent energy transfer from 58% to 31%–37%. Constraining the LHHL torsions has a negligible effect on energy transfer, presumably because their H-atom motions are not excited efficiently. Most of the initial energy transfer is to the peptide's torsional modes. With all the stretches and bends constrained the percent energy transfer decreases by a relatively small amount from 58% to 49%, which shows that more than 80% of the initial energy transfer is to the torsional modes. More energy is transferred to peptide rotation as modes are constrained and, thus, less energy is transferred to vibration. With no constraints the overall energy transfer is 58% with only 4% to rotation. However, with all the modes constrained there is no energy transfer to vibration, but 13% to rotation.

4. Summary

From this trajectory simulation the following has been determined concerning the dynamics of energy transfer in the activation of peptides by collisions with Ar.

For zero impact parameter, the energy transfer efficiency is near 75% at high E_{rel}, increasing from 40% as E_{rel} is increased from 20 kcal/mol. Such a change in energy transfer is consistent with a statistical type model at low E_{rel}, with a transition to impulsive energy transfer with increase in E_{rel}. In comparing the energy transfer efficiency for glycine and alanine polypeptides versus E_{rel} and peptide structure, energy transfer to the alanine peptides is less impulsive. This may be due to the presence of the methyl rotors for the alanine peptides, but more work needs to be done to reach a definitive conclusion.

The extended peptides have larger collision cross sections $\pi b_{max}^2$and smaller average energy transfer $\langle \Delta E \rangle$ than do the folded peptides. For both the folded and extended peptides the average energy transfer to vibration $\langle \Delta E_{vib} \rangle$ is larger than that to rotation $\langle \Delta E_{rot} \rangle$. The value of $\langle \Delta E_{rot} \rangle$ is similar for the extended and folded $(gly)_4$ peptides. However, the $\langle \Delta E_{vib} \rangle / \langle \Delta E_{rot} \rangle$ ratio is larger for the folded peptide than the extended one.

For collisions with an impact parameter of zero, the efficiency of energy transfer depends on peptide structure with the folded peptides more easily activated. This may arise from more multiple encounters between the peptide and the rare gas atom when it is folded. The effect of structure is less significant for the glycine than the alanine polypeptides, since the collisions are more impulsive for the former.

The collisions between the rare gas and the peptide initially deposits some energy in all the modes of the peptide, however there is some specificity in this energy transfer. The torsions receive most of the energy and the stretches receive the least. Energy transfer to the bends is also small and similar to that for the stretches.

Acknowledgement

This research was supported by the National Science Foundation.

References

[1] J.S. Klassen, P. Kerbale, J. Am. Chem. Soc. 119 (1997) 6552.
[2] E.M. Marzluff, S. Campbell, M.T. Rodgers, J.L. Beauchamp, J. Am. Chem. Soc. 116 (1994) 7787.
[3] E.M. Marzluff, S. Campbell, M.T. Rodgers, J.L. Beauchamp, J. Am. Chem. Soc. 116 (1994) 6947.
[4] A.J. Alexander, P. Thibault, R.K. Boyd, Int. J. Mass Spectrom. Ion Processes 98 (1990) 107.
[5] X. Cheng, C. Fenselau, Int. J. Mass Spectrom. Ion Processes 98 (1990) 107.
[6] R.R. Hudgins, Y. Mao, M.A. Ratner, M.F. Jarrold, Biophys. J. 76 (1999) 1591.
[7] D.E. Clemmer, R.R. Hudgins, M.F. Jarrold, J. Am. Chem. Soc. 117 (1995) 10141.
[8] D.G. Gross, P.D. Schnier, S.E. Rodriguez-Cruz, C.K. Fagerquist, E.R. Williams, Proc. Natl. Acad. Sci. USA 93 (1996) 3143.
[9] I.A. Kaltashov, C. Fenselau, Proteins Struct. Funct. Genet. 27 (1997) 165.
[10] J.S. Klassen, A. Blades, P. Kerbale, J. Phys. Chem. 99 (1995) 15509.
[11] S.J. Valentine, G. Anderson, A.D. Ellington, D.E. Clemmer, J. Phys. Chem. B 118 (1996) 8355.
[12] O. Meroueh, W.L. Hase, J. Phys. Chem. A 103 (1999) 3981.
[13] E. Marzluff, J.L. Beauchamp, Large Ions: Their Vaporization, Detection and Structural Analysis, Wiley, New York, 1996.
[14] R.G. Gilbert, M.M. Sheill, P. Derrick, J. Org. Mass Spectrom. 120 (1985) 430.
[15] K. Vekey, A. Gomory, Rapid Commun. Mass Spectrom. 119 (1990) 6552.
[16] A. Somogyi, V.H. Wysocki, I. Mayer, J. Am. Chem. Soc. 5 (1994) 704.
[17] K. Zhang, C.J. Cassady, A. Chung-Phillips, J. Phys. Chem. 116 (1994) 11512.
[18] Y.-D. Wu, D.-P. Wang, J. Am. Chem. Soc. 120 (1998) 13485.
[19] L. McCormack, Á. Somogyi, A.R. Dongré, V.H. Wysocki, Anal. Chem. 65 (1993) 2859.
[20] J. Los, T.R. Govers, Collision Spectroscopy, Plenum, New York, 1978.
[21] R. Weinkauf, W.E. Schlag, T.J. Martinez, R.D. Levine, J. Phys. Chem. 101 (1997) 7702.
[22] R. Dongré, J.L. Jones, Á. Somogyi, V.H. Wysocki, J. Am. Chem. Soc. 118 (1996) 8365.
[23] K. Zhang, D.M. Zimmerman, A. Chung-Phillips, C.J. Cassady, J. Am. Chem. Soc. 115 (1993) 10812.
[24] G. Harrison, T. Yalcin, Int. J. Mass Spectrom. Ion Processes 165 (1997) 339.
[25] T. Lenzer, K. Luther, Ber. Bunsen-Ges. Phys. Chem. 101 (1997) 581.
[26] R.G. Gilbert, K.F. Lim, J. Phys. Chem. 94 (1990) 78.
[27] G. Lendvay, G.C. Schatz, J. Chem. Phys. 98 (1993) 1034.
[28] K. Bolton, S. Nordholm, Chem. Phys. 103 (1996) 206.
[29] B.M. Toselli, J.R. Barker, J. Chem. Phys. 97 (1992) 1809.
[30] A. Linhananta, K.F. Lim, Phys. Chem. Chem. Phys. 1 (1999) 3467.
[31] W.L. Hase, R.J. Duchovic, X. Hu, A. Komornicki, K.F. Lim, D.-H. Lu, G.H. Peslherbe, K.N. Swamy, S.R. Vande Linde, A. Varandas, H. Wang, R.J. Wolf, QCPE 16 (1996) 671.
[32] W.D. Cornell, P. Cieplak, C.I. Bayly, I.R. Gould, K.M. Merz Jr., D.M. Ferguson, D.C. Spellmeyer, T. Fox, J.W. Caldwell, P.A. Kollman, J. Am. Chem. Soc. 117 (1995) 5179.
[33] S. Chapman, D.L. Bunker, J. Chem. Phys. 62 (1975) 2890.
[34] S. Sloane, W.L. Hase, J. Chem. Phys. 66 (1977) 1523.
[35] Y.H. Cho, S.R. Vande Linde, L. Zhu, W.L. Hase, J. Chem. Phys. 96 (1992) 8275.
[36] T.D. Sewell, D.L. Thompson, Int. J. Mod. Phys. B 11 (1997) 1067.
[37] G.H. Peslherbe, H. Wang, W.L. Hase, in Advances in Chemical Physics, Monte Carlo Methods in Chemical Physics Vol. 105, D.M. Ferguson, J.I. Siepmann, D.G. Truhlar (Eds.), Wiley, New York, 1999, p. 171.
[38] H.A. Laitinen, Chemical Analysis, McGraw-Hill, New York, 1960.
[39] M. Takano, T. Yamato, J. Higo, A. Suyama, K. Nagayama, J. Am. Chem. Soc. 121 (1999) 605.
[40] T. Baer, W.L. Hase, Unimolecular Reaction Dynamics. Experiment and Theory, Oxford, New York, 1996.
[41] S. Nordholm, Ber. Bunsenges. Phys. Chem. 101 (1997) 574.
[42] A.R. Whyte, K.F. Lim, R.G. Gilbert, W.L. Hase, Chem. Phys. Lett. 152 (1988) 377.
[43] Other approaches for determining b_{max} are discussed in X. Hu, W.L. Hase, J. Phys. Chem. 98 (1998) 4040; K.F. Lim, R.G. Gilbert, ibid. 94 (1990) 72; G. Lendvay, G.C. Schatz, J. Chem. Phys. 96 (1992) 3753.
[44] W.L. Hase, C.L. Darling, L. Zhu, J. Chem. Phys. 96 (1992) 8295.